WATER RESOURCES RESEARCH, VOL. 31, NO. 9, PAGES 2253–2261, SEPTEMBER 1995

Steam stripping of contaminated unsaturated zone of subsoils: Theoretical model of start-up phase

H. J. H. Brouwers and Shuanhu Li

Department of Civil Engineering and Management, University of Twente, Enschede, Netherlands

Abstract. The present paper addresses the unsteady process of steam stripping of the unsaturated zone of soils contaminated with volatile nonaqueous phase liquids. First, on the basis of Darcy's law and the conservation laws of mass and energy, a one-dimensional model is derived for the propagation of the steam front in the start-up phase. It is shown that this process is governed by one dimensionless group y. Subsequently, the evaporation mechanism behind, the transport to, and the condensation at the front of volatile contaminants are considered, taking the view that nonequilibrium exists between liquid and vapor phases. The model leads to a moving boundary problem which is of special mathematical interest. By a suitable transformation of the governing partial differential equations, the problem is brought into a fixed domain and solved numerically. For a broad range of the governing dimensionless numbers, computation results are presented. The results obtained in this paper make clear the role of the prevailing principal physical phenomena during the start-up phase of the process.

Introduction

Volatile organic compounds (VOCs) are among the most ubiquitous soil contaminants. Though most of these liquids are immiscible with water (often referred to as nonaqueous phase liquids, NAPLs), they have aqueous phase solubilities that substantially exceed drinking water standards (Table 1). Contamination of the unsaturated zone by VOCs and their transport to the groundwater has therefore become one of the major environmental problems in most industrialized countries. Hence, lately, considerable effort has been devoted to the cleanup of sites contaminated with VOCs.

Current remediation mostly issues from excavation and cleaning or dumping of the contaminated soil. As these procedures are expensive, and sometimes even dangerous, alternative concepts and techniques are needed. A cheap and efficient way of cleaning up the soil is offered by in situ remediation. In situ cleaning techniques avoid the cost of excavation, transportation, and possible demolishment of buildings, roads, and so on and are therefore attractive from a cost point of view. An in situ remediation is usually started by skimming or the pumping up of groundwater and nondissolved contaminant, followed by an above ground treatment. Subsequently, the portion of remaining dissolved contaminant is removed from soil and groundwater by evaporative techniques. Usually, air, water, or steam are employed as stripping media. Enhanced and accelerated cleaning is achieved at elevated temperatures. Hence the use of hot media, such as steam and heated air, can be attractive as short cleaning times are often beneficial, for instance, at sites in commercial use.

In order to optimize in situ cleaning, physical models are required which represent an adequate description of the prevailing processes. To the authors' knowledge the first publication on in situ soil cleaning with steam was by *Maas* [1982]. Subsequently, analyses and experiments of the process were presented by *Hilberts* [1986], *Vreeken and Sman* [1988], *Hunt et al.* [1988a, b], *Udell and Stewart* [1990], and *Falta et al.* [1992a, b]. These elaborations assumed constant steam injection rates and steady steam-front velocities. Furthermore, all previous studies started from local equilibrium between liquid and vapor phases of the contaminant, though it is recognized that in a large number of practical situations this simplification are not allowed. *Yuan and Udell* [1993] developed a nonequilibrium model for the distillation of a free NAPL. For free NAPL the concentration at the liquid-vapor interface is constant (and proportional to the vapor pressure of the pure contaminant).

The present paper addresses the start-up phase of the steam-stripping process whereby the liquid contaminant concentration is below the solubility limit of the present water. Constant pressure injection of steam into an unsaturated matrix is considered. The steam-front propagation is obtained by employing Darcy's law and an energy balance. The model allows for the condensation heat liberated at the front and heat transported away by axial conduction to the surroundings. The resulting analytic expression reveals that axial heat conduction plays a major role of importance, its neglect being allowed only in some limiting cases.

Subsequently, the unsteady evaporation and convective transport of contaminant behind the front and its deposition at the front is addressed thoroughly. To describe the transport of the contaminant, a nonequilibrium model is proposed. As the liquid contaminant concentration is below the solubility limit, it decreases as contaminant is removed from the water. Hence the contaminant concentration at the liquid-vapor interface depends on the liquid contaminant concentration (by Henry's law). This feature of the process results in a coupling of liquid and vapor contaminant concentrations. Numerical solutions of the governing partial differential equations illustrate the influence of the governing dimensionless numbers.

Steam Flow

In this section the one-dimensional and unsteady propagation of the steam front in the soil is analyzed. The soil is

Paper number 95WR01270.
0043-1397/95/95WR-01270$05.00

Table 1. Maximum Water Solubilities and Drinking Water Concentrations of Benzene and Ethylene Dibromide at 20°C

Substance	Maximum Water Solubility, mg/L	Maximum Drinking Water Concentration, mg/L
Benzene	1780	0.005
Ethylene dibromid	4.3	0.005

Taken from *Miller et al.* [1990].

considered as a homogeneous and isotropic porous medium and is considered to have a constant thickness and to be confined by impermeable and adiabatic top and bottom layers. The process involves the displacement of air by water vapor, with condensation of the water vapor and release of latent heat. This heat is used to heat up the soil and the initial groundwater.

Throughout this paper it is assumed that the water saturation S_l is smaller than irreducible (connate) water saturation S_{ir}, so that this liquid water is immobile. This water saturation consists of two parts, namely, the initial water saturation S_{l0} and the condensation water saturation S_{lc}. Thus it is assumed that

$$S_{lc} + S_{l0} < S_{ir}. \tag{1}$$

It should be noted that the assumption expressed by (1) is applicable because S_{ir} amounts to 15–25% in soils [*Buchlin and Stubos*, 1991] and initial water and condensate can obey (1) in the unsaturated zone. Moreover, the water movement can also be neglected if the water saturation is not too far above S_{ir}. At the end of this section an explicit expression for S_{lc} is obtained.

The steam is injected at $x = 0$ at a constant pressure. The steam flows through the unsaturated matrix to the condensation front (Figure 1), the position of the front designated by $X_0(t)$, where the ambient pressure P_0 prevails. Condensation occurs at the front until the soil and the initial groundwater are heated up to the saturation temperature of the steam. The pressure drop between injection point and condensation front (typically 0.1 bar) is much smaller than the absolute pressure in the porous medium (ambient pressure), so that the saturation temperature T_{sat} may be regarded as constant. Hence behind the steam front ($0 \le x \le X_0$) the temperature of the mixture of soil, water, and steam equals T_{sat}. Furthermore, the analysis is restricted to a one-dimensional representation of the process by assuming the process to be uniform through the height of the porous medium.

The first step in the analysis is to consider the mass and momentum balances of the vapor flow. The steam flow to the front and air flow ahead of the front obey Darcy's law

$$\frac{X_0 u_v \eta_v}{\kappa \kappa_{rv}} + \frac{(L - X_0) u_{air} \eta_{air}}{\kappa \kappa_{rair}} = P_{in} - P_0. \tag{2}$$

where it has been assumed that the vapor displaces the air evenly.

An overall mass balance of injected water vapor, accumulated condensate, and water vapor behind the front yields

$$u_v \rho_v = (\rho_l S_{lc} \phi + \rho_v S_v \phi) \frac{dX_0}{dt}. \tag{3}$$

Similarly, an overall mass balance of the section ahead of the front gives

$$u_{air} = S_{air} \phi \frac{dX_0}{dt}. \tag{4}$$

Note that by definition

$$S_v = 1 - S_{l0} - S_{lc}, \tag{5}$$

and

$$S_{air} = 1 - S_{l0}. \tag{6}$$

Equations (2)–(4) are now combined, and then it is assumed that the flow is condensation dominated. The amount of condensed water will be much larger than the amount of vapor in the pores, that is,

$$\rho_l S_{lc} \gg \rho_v S_v. \tag{7}$$

It is furthermore assumed

$$X_0 \eta_v \rho_l S_{lc} \gg (L - X_0) \eta_{air} \rho_v S_{air}. \tag{8}$$

This inequality states that the resistance to the vapor flow is much larger than to the air flow. This assumption is reasonable as the air velocity, which is equal to the steam-front velocity, is much smaller than the vapor flow to the front. It is erroneous at the beginning of the process since then the length of the air-saturated column is largest, namely, L, and the distance between entrance and front, governed by X_0, is nearly zero. Equations (2)–(4), (7), and (8) result in

$$\rho_l S_{lc} \phi \frac{dX_0}{dt} = \frac{\kappa_{rv} \kappa}{\nu_v} \frac{P_{in} - P_0}{X_0}, \tag{9}$$

which is the balance equation for the flow process. Strictly speaking, (8) is not applicable at the beginning of the process since

$$X_0|_{t=0} = 0. \tag{10}$$

When the amount of formed condensate is sufficiently large, the error induced by the assumptions (7) and (8) is acceptable. This has to be verified a posteriori.

A special case can be considered where the ambient air is displaced by another noncondensable. For example, if the ambient air is displaced by injected air ($\eta_v = \eta_{air}$ then holds), and therefore $S_{lc} = 0$; it follows from (3)–(6) that $u_v = u_{air}$ and $S_v = S_{air}$. Equation (2) yields as the gas velocity

$$u_{air} = \frac{\kappa_{rair} \kappa}{\eta_{air}} \frac{P_{in} - P_0}{L}, \tag{11}$$

which is constant. The position of the front is then obtained by integrating (4) and applying initial condition (10)

$$X_0 = \frac{u_{air}}{S_{air} \phi} t. \tag{12}$$

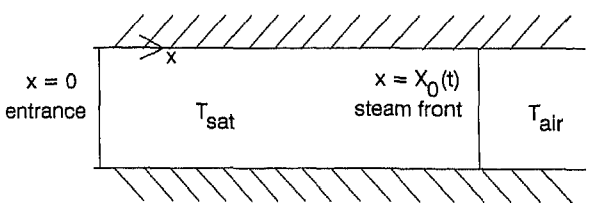

Figure 1. Schematic representation of the process.

These equations have been used by *Bird et al.* [1960, example 22.6-2] in considering the special case of an entering fluid into a porous bed. This fluid contains a dilute component which is adsorbed at the solid bed. Since the adsorbed component is dilute, the velocity of the entering carrier fluid and the displacement front were considered as constant. Here a substantial part of the entering vapor condenses at the steam front, implying essentially different conditions than encountered by *Bird et al.* [1960].

For the case at hand, condensation occurs at the front; additional information is then needed to determine the position of the front. This information is provided by an energy balance at the front. An analysis of latent heat that is liberated at the condensation front and heat thermally conducted away ahead of the front yields

$$\rho_l S_{lc} \phi H_{lat} \frac{dX_0}{dt} = -\bar{k}_s \left.\frac{\partial T_{air}}{\partial x}\right|_{x=X_0}. \tag{13}$$

Ahead of the steam front ($X_0 \le x \le \infty$), the temperature of soil, groundwater, and air, denoted by $T_{air}(x, t)$, has to be assessed in order to determine the right-hand side of (13). This temperature increases due to axial heat conduction. The energy equation of this region reads

$$\overline{\rho_s c_{ps}} \frac{\partial T_{air}}{\partial t} = \bar{k}_s \frac{\partial^2 T_{air}}{\partial x^2}, \tag{14}$$

where $\bar{k}_s$ and $\overline{\rho_s c_{ps}}$ represent the thermal conductivity and heat capacity, respectively, of the mixture of soil, (initial) groundwater, and air. In deriving (14) it has been assumed that the heat transported by conduction is dominant over the convective heat transfer, that is,

$$\bar{k}_s \frac{\partial^2 T_{air}}{\partial x^2} \gg u_{air} \rho_{air} c_{pair} \frac{\partial T_{air}}{\partial x}, \tag{15}$$

which will be verified later.

Equation (14) holds in the region $X_0 \le x \le \infty$ and is subject to initial condition

$$T_{air}|_{t=0} = T_0. \tag{16}$$

As boundary conditions prevail,

$$T_{air}|_{x=X_0} = T_{sat}, \tag{17}$$

$$T_{air}|_{x=\infty} = T_0. \tag{18}$$

In (16) and (18), T_0 denotes the initial temperature of the porous medium. Solving (14) subject to (16)–(18) leads to

$$T_{air}(x, t) = \gamma_2 + \gamma_1 \int_{\eta=0}^{x/t^{1/2}} \exp\left[-\frac{1}{4a_1}\eta^2\right] d\eta \tag{19}$$

where

$$a_1 = \bar{k}_s / \overline{\rho_s c_{ps}} \tag{20}$$

and γ_1 and γ_2 satisfy

$$\gamma_2 + \gamma_1 \int_{\eta=0}^{\infty} \exp\left[-\frac{1}{4a_1}\eta^2\right] d\eta = T_0 \tag{21}$$

and

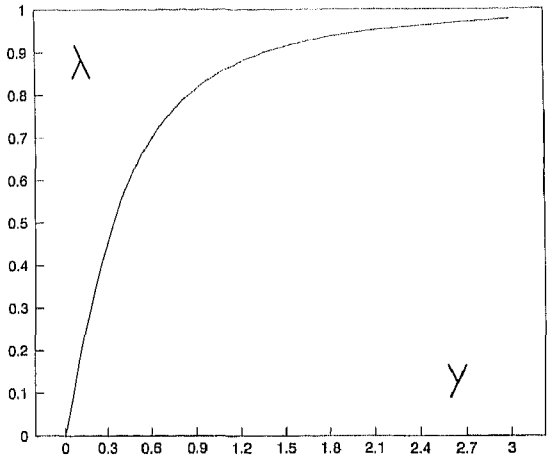

Figure 2. Solution of $\lambda(y)$.

$$\gamma_2 + \gamma_1 \int_{\eta=0}^{X_0/t^{1/2}} \exp\left[-\frac{1}{4a_1}\eta^2\right] d\eta = T_{sat}. \tag{22}$$

Combining (9), (13), and (19)–(22) yields

$$a_2 = 2a_1 \frac{\dfrac{X_0}{t^{1/2}} \exp\left[-\dfrac{1}{4a_1}\left(\dfrac{X_0}{t^{1/2}}\right)^2\right]}{\displaystyle\int_{X_0/t^{1/2}}^{\infty} \exp\left[-\frac{1}{4a_1}\eta^2\right] d\eta}, \tag{23}$$

where

$$a_2 = \frac{2\kappa_{rw}\kappa H_{lat}(P_{in} - P_0)}{\nu_w \overline{\rho_s c_{ps}}(T_{sat} - T_0)}. \tag{24}$$

Note that the left-hand side of (23) is a constant. This implies that $X_0/t^{1/2}$ must be a constant as well. Accordingly,

$$X_0/t^{1/2} = a_2^{1/2}\lambda \tag{25}$$

is substituted into (23), yielding

$$\pi^{1/2} y \operatorname{erfc}(\lambda y) e^{\lambda^2 y^2} = \lambda. \tag{26}$$

In (26) the following dimensionless group is introduced:

$$y = \left(\frac{a_2}{4a_1}\right)^{1/2} \equiv \left(\frac{\kappa_{rw}\kappa H_{lat}(P_{in} - P_0)}{2\nu_w \bar{k}_s (T_{sat} - T_0)}\right)^{1/2}, \tag{27}$$

and $\operatorname{erfc}(x)$, the complement error function, is defined as

$$\operatorname{erfc}(x) = 1 - \operatorname{erf}(x) = 1 - \frac{2}{\pi^{1/2}} \int_{\eta=0}^{x} \exp(-\eta^2)\, d\eta. \tag{28}$$

For a given y, which is governed by a_1 and a_2, λ can be determined as the root $\lambda(y)$ of (26). Furthermore, the steam-front position then follows from (25). Thus it is sufficient to know how $\lambda(y)$ changes versus y. For a more detailed study of (26) the reader is referred to *Gilding and Li* [1995]. As it is not possible to give an analytic expression of $\lambda(y)$ in terms of y, the bisection method is used to compute $\lambda(y)$ numerically, the result being depicted in Figure 2. The numerical results for similar equations (also containing combinations of erf, erfc, and exp), stemming from melting and freezing problems, can

be found in the standard work of *Carslaw and Jaeger* [1959, chapter 11].

Now a few physical remarks are required. The dimensionless group y is a measure for the latent heat transport by vapor flow divided by the heat conducted away ahead of the front. The fact that $\lambda(0) = 0$ states that the steam front stagnates when there is no vapor flow (or infinitely large heat loss by heat conduction). On the other hand, Figure 2 shows that $\lambda \to 1$ when $y \to \infty$. That is, $\lambda = 1$ when the thermal conductivity (or resistance to vapor flow) is negligibly small. For this particular case the following applies:

$$X_0 = (a_2 t)^{1/2}. \tag{29}$$

This corresponds to the case where all liberated latent heat is used for the heating up of soil and initial groundwater:

$$\rho_v u_v H_{\text{lat}} = \overline{\rho_s c_{ps}}(T_{\text{sat}} - T_0)\frac{dX_0}{dt}. \tag{30}$$

By combination of (3), (7), (9), and (24) it follows that

$$dX_0/dt = a_2/2X_0. \tag{31}$$

Solving (31) subject to the initial condition (10) indeed yields (29). It can be seen that for this case, λ approximates unity and the steam front attains the highest speed (equations (25) and (26) and Figure 2).

Finally, to verify whether S_{lc} satisfies conditions (7) and (8), the amount of condensed water is determined. This is allowed as assumptions (7) and (8) cause an underestimation of S_{lc}. The amount of condensed water follows from (9), (24), and (25):

$$S_{lc} = \frac{\overline{\rho_s c_{ps}}(T_{\text{sat}} - T_0)}{H_{\text{lat}}\phi\lambda^2\rho_l}. \tag{32}$$

Equation (32) reveals that the amount of condensed steam does not depend on the position of the front. Hence the water saturation behind the front, which consists of S_{l0} and S_{lc}, is constant. Furthermore, the relative permeability κ_{rv}, which depends on S_l, is therefore also constant. Equation (32) also implies that the amount of condensate is least for $\lambda = 1$, that is, the case whereby all latent heat is available for heating up the porous medium at the steam front and conductive losses ahead of the front are negligible.

In order to verify (15), it is combined with (4) and (19)–(22) yielding

$$\overline{\rho_s c_{ps}} \gg S_{\text{air}}\rho_{\text{air}}c_{p\text{air}}\phi, \tag{33}$$

a condition which is fulfilled in most practical cases.

Contaminant Transport

In this section the water vapor flow is used to assess the evaporation and transport of the contaminant in the soil. A common assumption made in the chemical engineering field is that the mass transfer between liquid and vapor contaminant is represented by the difference between equilibrium and actual concentration.

For the vapor phase, neglecting diffusion and dispersion, a differential mass balance of transported, accumulated, and evaporated contaminant gives

$$u_v\frac{\partial C_v}{\partial x} + \phi S_v\frac{\partial C_v}{\partial t} = g_t(HC_l - C_v). \tag{34}$$

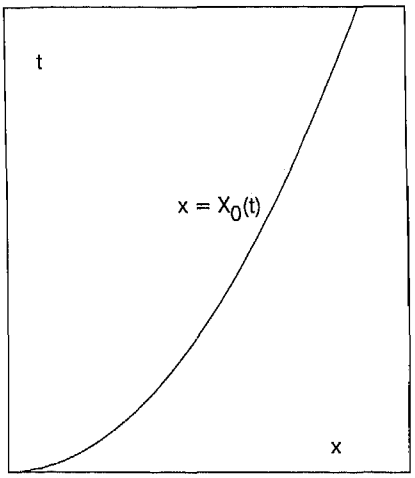

Figure 3a. Moving boundary problem.

S_v is provided by (5) and H reflects the dimensionless Henry's law coefficient

$$H = \frac{P_{p,\text{sat}}(T_{\text{sat}})M_p}{RT_{\text{sat}}C_{lm}}. \tag{35}$$

The mass balance of the contaminant in the water phase is governed by

$$\phi(S_{l0} + S_{lc})\frac{\partial C_l}{\partial t} = -g_t(HC_l - C_v). \tag{36}$$

Equation (36) does not include sorption. However, if linear sorption is assumed, the nature of (34) and (36) would not change.

Equations (4) and (36), which are valid in the region $t \geq 0$ and $0 \leq x \leq X_0(t)$ (Figure 3a), form a moving boundary problem. In order to bring this problem into a fixed domain and prepare this set of equations for numerical treatment, the following coordinate transformation is introduced:

$$\tilde{t} = \frac{X_0(t) - x}{L}, \tag{37}$$

$$\tilde{x} = x/L. \tag{38}$$

Furthermore, to set (34) and (36) dimensionless, the following variables are introduced:

$$\tilde{C}_l = C_l/C_{lm}, \tag{39}$$

$$\tilde{C}_v = C_v\rho_l/C_{lm}\rho_v. \tag{40}$$

The front position $X_0(t)$ follows from (25). Equations (34) and (36) in terms of the variables $\tilde{C}_l$, $\tilde{C}_v$, $\tilde{t}$, and $\tilde{x}$, application of (3) and (7), and using (24) and (32) to eliminate λ^2 and a_2 yields

$$\frac{\partial\tilde{C}_v}{\partial\tilde{t}} - \frac{\partial\tilde{C}_v}{\partial\tilde{x}} = Me(\tilde{t} + \tilde{x})(\tilde{C}_v - \tilde{H}\tilde{C}_l), \tag{41}$$

$$\partial\tilde{C}_l/\partial\tilde{t} = \beta Me(\tilde{t} + \tilde{x})(\tilde{C}_v - \tilde{H}\tilde{C}_l), \tag{42}$$

with

$$\beta = \frac{S_{lc}}{S_{lc} + S_{l0}}, \tag{43}$$

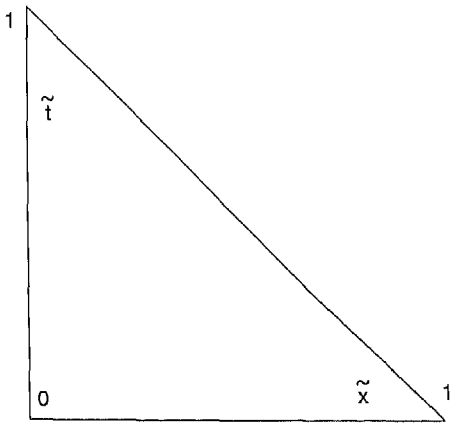

Figure 3b. Fixed domain.

$$Me = \frac{\eta_v L^2 g_t}{\kappa_{rv}\kappa(P_{in} - P_0)}, \tag{44}$$

$$\tilde{H} = \rho_l H/\rho_v. \tag{45}$$

The hyperbolic system (41) and (42) holds in the triangular domain $0 < \tilde{t} < 1$, $0 < \tilde{x} < 1$ and $\tilde{t} + \tilde{x} < 1$ (Figure 3b).

Note that β represents the ratio of amount of condensate and total amount of water (initial water plus condensate). *Me* represents the Merkel number. This dimensionless number constitutes the ratio of mass transfer rate and fluid velocity (in steady state situations the fluid velocity is governed, namely, by $\kappa_{rv}\kappa(P_{in} - P_0)/\eta_v L$).

In order to form a well-posed problem and solve (41) and (42), boundary (initial) conditions on $\tilde{t}$ and $\tilde{x}$ have to be specified. First, it should be observed that the system is of a hyperbolic type. $\bar{C}_v$ can be expressed in terms of $\bar{C}_l$ and $\partial\bar{C}_l/\partial\tilde{t}$ with the help of (42). Eliminating $\bar{C}_v$ from (41) yields a hyperbolic differential equation for $\bar{C}_l$. A standard analysis then reveals that the two characteristics of the system are $\tilde{x} = \text{const}$ and $\tilde{x} + \tilde{t} = \text{const}$. It is well-known that characteristics play a major role in studying how well the hyperbolic equations of second order are posed. For general references, see the books by *Courant and Hilbert* [1953] and *Zauderer* [1989].

It is interesting to realize that two boundaries of the domain, $\tilde{x} = 0$ and $\tilde{x} + \tilde{t} = 1$, coincide with the characteristics of the hyperbolic system. Thus the hyperbolic system (41) and (42) can be solved by the usual technique of integration along the characteristic and linear iteration if a boundary condition for $\bar{C}_v$ on $\tilde{x} = 0$ and an "initial" condition at $\tilde{t} = 0$ are specified. These conditions are derived below.

At the entrance (i.e., $\tilde{x} = 0$) the contaminant concentration of the entering steam is known. For clean steam the boundary condition reads

$$\bar{C}_v(0, \tilde{t}) = 0. \tag{46}$$

Subsequently, a relation between $\bar{C}_v$ and $\bar{C}_l$ for $\tilde{t}$ will be specified in the following.

The liquid contaminant concentration consists of two parts, namely, the initial liquid contaminant concentration C_{l0} (based on initial water saturation S_{l0}) and the contaminant which is evaporated behind the front and condensed at the front. An overall mass balance of contaminant gives

$$\phi \int_{x=0}^{X_0} (C_l(S_{lc} + S_{l0}) - C_{l0}S_{l0})\, dx = -\phi \int_{x=0}^{X_0} C_v S_v\, dx + \int_{t=0}^{t} u_v C_v(0, t)\, dt. \tag{47}$$

Differentiating with respect to t yields

$$\phi(C_l(X_0, t)(S_{lc} + S_{l0}) - C_{l0}S_{l0})\frac{dX_0}{dt} + \phi C_v(X_0, t)S_v\frac{dX_0}{dt} = -\phi \int_{x=0}^{X_0} \left(S_v\frac{\partial C_v}{\partial t} + (S_{l0} + S_{lc})\frac{\partial C_l}{\partial t}\right) dx + u_v C_v(0, t). \tag{48}$$

Setting the left-hand sides of (34) and (36) equal, substituting the result into the integral of (48), and integrating yields

$$\phi(C_l(X_0, t)(S_{lc} + S_{l0}) - C_{l0}S_{l0})\frac{dX_0}{dt} = -\phi C_v(X_0, t)S_v\frac{dX_0}{dt} + u_v C_v(X_0, t). \tag{49}$$

Substituting (3), (49) is written with (39) and (40) in transformed variables as

$$\bar{C}_l(\tilde{x}, 0) = \bar{C}_{l0}(1 - \beta) + \beta\bar{C}_v(\tilde{x}, 0), \tag{50}$$

wherein (43) has been inserted. The liquid contaminant concentration at the front consists of the initial and condensed contaminant. Equation (50) describes the liquid contaminant concentration at the front as a function of the (dimensionless) initial contaminant concentration $\bar{C}_{l0}$ ($= C_{l0}/C_{lm}$, $0 \le \bar{C}_{l0} \le 1$), diluted by the condensed water, and the vapor contaminant concentration, represented by $\bar{C}_v(\tilde{x}, \tilde{t} = 0)$. Equations (41), (42), (46), and (50) form a complete system, and thus, in the following section, numerical solutions of this system are presented.

Numerical Solution

In this section a numerical solution procedure for the governing equations of the previous section is derived. As mentioned in the previous section, the two characteristics of coupled (41) and (42) are $\tilde{x} = \text{const}$ and $\tilde{x} + \tilde{t} = \text{const}$. It is therefore natural to employ the method of characteristics to determine the solution of the system. For this method it is essential to make use of the fact that the system can be written in terms of the total differential of $\bar{C}_l$ and $\bar{C}_v$ along the characteristics [see *Burden et al.*, 1978]. A uniform mesh, as depicted in Figure 4, is chosen for the triangular domain. Let n be the number of steps, then the distance between adjacent discretization points δ follows from

$$\delta = \frac{1}{n}. \tag{51}$$

The discretisation points $(\tilde{x}, \tilde{t})$ which are situated on the intersections of the lines $\tilde{x} + \tilde{t} = j\delta$ and $\tilde{x} = i\delta$ are denoted by $(i\delta, (j - i)\delta)$, with $i = 0, 1, \cdots, j$ and $j = 0, 1, \cdots, n$. For convenience, the following notations are introduced:

$$\bar{C}_v^{i,j-i} = \bar{C}_v[i\delta, (j - i)\delta], \tag{52}$$

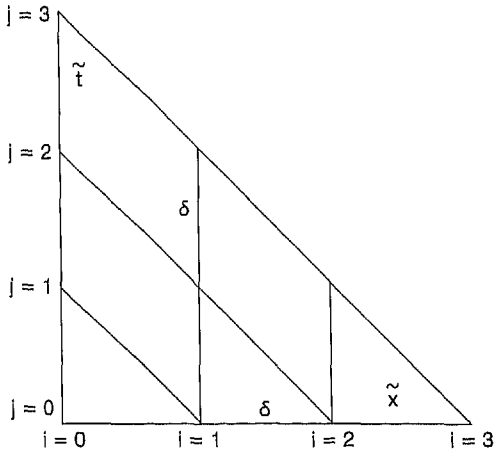

Figure 4. Discretization points ($n = 3$ as example).

$$\tilde{C}_l^{i,j-i} = \tilde{C}_l[i\delta, (j-i)\delta]. \tag{53}$$

Note that along the characteristic $\tilde{x} + \tilde{t} = \text{const}$ and $\tilde{x} = \text{const}$ hold

$$\frac{D\tilde{C}_v}{D\tilde{x}} = \frac{\partial \tilde{C}_v}{\partial \tilde{x}} - \frac{\partial \tilde{C}_v}{\partial \tilde{t}}, \tag{54}$$

and

$$D\tilde{C}_l/D\tilde{t} = \partial \tilde{C}_l/\partial \tilde{t}, \tag{55}$$

respectively, where D denotes total differentiation. Thus discretising of (41) and (42) at point $(i\delta, (j-i)\delta)$ using the properties of the characteristics the following schemes are obtained:

$$\tilde{C}_v^{i,j-i} = \tilde{C}_v^{i-1,j-i+1} - \tau_j Me(\tilde{C}_v^{i,j-i} - \tilde{H}\tilde{C}_l^{i,j-i}), \tag{56}$$

$$\tilde{C}_l^{i,j-i} = \tilde{C}_l^{i,j-i-1} + \tau_j \beta Me(\tilde{C}_v^{i,j-i} - \tilde{H}\tilde{C}_l^{i,j-i}), \tag{57}$$

with

$$\tau_j = j\delta^2. \tag{58}$$

Equations (56) and (57) can easily be rewritten to obtain $\tilde{C}_v^{i,j-i}$ and $\tilde{C}_l^{i,j-i}$ explicitly in terms of $\tilde{C}_v^{i-1,j-i+1}$ and $\tilde{C}_l^{i,j-i-1}$. Hence using the schemes $\tilde{C}_v^{0,j}$ must be specified. This is supplied by boundary condition (46). At the boundary $\tilde{t} = 0$, initial condition (50) has to be satisfied

$$\tilde{C}_l^{j,0} = \tilde{C}_{l0}(1-\beta) + \beta \tilde{C}_v^{j,0}. \tag{59}$$

Discretising (41) along the characteristic $\tilde{x} + \tilde{t} = j\delta$ at $(j\delta, 0)$ yields

$$\tilde{C}_v^{j,0} = \tilde{C}_v^{j-1,1} - \tau_j Me(\tilde{C}_v^{j,0} - \tilde{H}\tilde{C}_l^{j,0}). \tag{60}$$

This equation follows in fact from (56) with $i = j$ substituted. Combining (59) and (60) yields

$$\tilde{C}_v^{j,0} = \frac{\tilde{C}_v^{j-1,1} + \tilde{H}\tau_j Me\tilde{C}_{l0}(1-\beta)}{\tau_j Me(1-\beta\tilde{H}) + 1}. \tag{61}$$

Accordingly, $\tilde{C}_v^{j,0}$ and $\tilde{C}_l^{j,0}$ can be obtained in terms of $\tilde{C}_v^{j-1,1}$ with the help of (59) and (61). It is interesting to note that $j\delta \leq 1$ and that the positivity of $\tilde{C}_v^{j,0}$ requires that

$$n > Me(\beta\tilde{H} - 1), \tag{62}$$

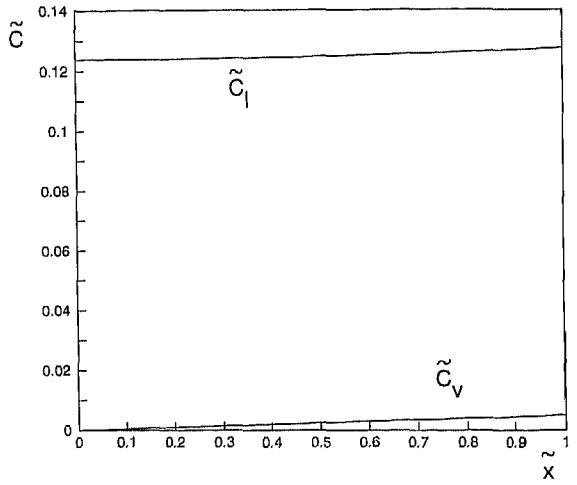

Figure 5. Dimensionless liquid contamination $\tilde{C}_l$ and vapor contamination $\tilde{C}_v$ at the end of the process, $\tilde{C}_{l0} = 0.25$, $\tilde{H} = 40$, $\beta = 0.5$, and $Me = 10^{-3}$.

which is a condition for a minimum number of discretization points. Using (56)–(61), the equations can readily be solved numerically.

Computational Results

In this section, solutions of the governing equations are presented for a number of cases of practical interest. Of particular interest are the values of $\tilde{C}_l$ and $\tilde{C}_v$ on the boundary $\tilde{x} + \tilde{t} = 1$. This line corresponds, namely, to $X_0 = L$, that is, when the front has attained the withdrawal well, implying the end of the unsteady process considered here (after the front has attained the withdrawal well, the vapor flow becomes constant and is governed by $\kappa_{rv}\kappa(P_{in} - P_0)/\eta_v L$).

Values of $\tilde{C}_l(0 \leq \tilde{x} \leq 1, \tilde{t} = 1 - \tilde{x})$ and $\tilde{C}_v(0 \leq \tilde{x} \leq 1, \tilde{t} = 1 - \tilde{x})$ against $\tilde{x}$ are depicted in Figure 5 for $\tilde{C}_{l0} = 0.25$, $\tilde{H} = 40$, $\beta = 0.5$, and $Me = 10^{-3}$. In Figure 6 the corresponding results of the computation with all values unaltered,

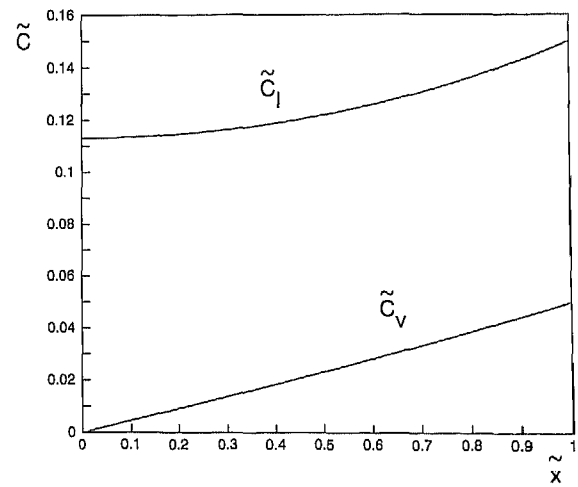

Figure 6. Dimensionless liquid contamination $\tilde{C}_l$ and vapor contamination $\tilde{C}_v$ at the end of the process, $\tilde{C}_{l0} = 0.25$, $\tilde{H} = 400$, $\beta = 0.5$, and $Me = 10^{-3}$.

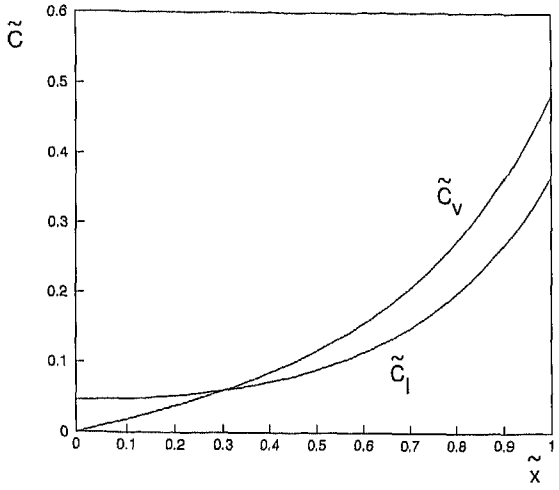

Figure 7. Dimensionless liquid contamination $\tilde{C}_l$ and vapor contamination $\tilde{C}_v$ at the end of the process, $\tilde{C}_{l0} = 0.25$, $\tilde{H} = 40$, $\beta = 0.5$, and $Me = 10^{-1}$.

except $\tilde{H} = 400$, are shown. All computations were performed with $n = 500$, so that (62) is satisfied.

Figures 5 and 6 illustrate the increase of $\tilde{C}_v$ in the positive $\tilde{x}$ direction, that is, the direction of flow. Figures 5 and 6 furthermore confirm the expected decrease of liquid contaminant. At the entrance (i.e., $\tilde{x} = 0$), this decrease is most pronounced. It should be noted that at the entrance the contaminant concentration, after dilution by condensation of pure water, is reduced to $\tilde{C}_{l0}(1 - \beta)$ (see equations (46) and (50)) and amounts to 0.125.

The contaminant removed near the entrance, where the steam front passes by first, is transported and deposited in the direction of the withdrawal well. Indeed, the liquid contaminant concentration there exceeds the (diluted) contaminant level of 0.125. At the exit, $x = X_0 = L$, $\tilde{C}_v(\tilde{x} = 1, \tilde{t} = 0)$, and $\tilde{C}_l(\tilde{x} = 1, \tilde{t} = 0)$ are related by (50). Evidently, during the start-up phase of the process, contaminant is not yet removed from the porous medium (as steam is not yet leaving the porous medium) but is carried from one place to the other. Actually, this feature follows from the imposed plug flow of steam and contaminant.

Comparing Figures 5 and 6 confirms that the evaporation and transport of contaminant are less if $\tilde{H}$ is smaller. This would be expected as a greater $\tilde{H}$ implies a higher contaminant vapor pressure and consequently a better evaporative behavior. An exploratory computation performed with $\tilde{H} = 4$ revealed that for this small $\tilde{H}$ value, $\tilde{C}_l(0 \leq \tilde{x} \leq 1, \tilde{t} = 1 - \tilde{x}) \cong 0.125$ and $\tilde{C}_v(0 \leq \tilde{x} \leq 1, \tilde{t} = 1 - \tilde{x}) \cong 0$, implying practically no mass has been transported. In this case, the contaminant remains homogeneously distributed in the soil, remaining at the initial contamination level, diluted by pure water condensation, and amounting to $\tilde{C}_{l0}(1 - \beta)$. The common assumption of an even contaminant concentration at the start of the steady state process is then allowed.

In Figure 7 the computational results pertaining to $\tilde{C}_{l0} = 0.25$, $\tilde{H} = 40$, $\beta = 0.5$, and $Me = 10^{-1}$ are depicted, and in Figure 8 those for $\tilde{H} = 400$ and all other values are unchanged. Comparing Figure 5 with Figure 7 and Figure 6 with Figure 8 one can readily see the enhanced mass transfer between liquid and vapor phases if Me is increased from 10^{-3} to 10^{-1}. Figures 7 and 8 illustrate the more pronounced transport of contaminant from the entrance region to the exit region. Figures 7 and 8 also confirm that the contaminant transport is enhanced as $\tilde{H}$ is increased.

Figure 7 reveals that $\tilde{C}_v$ exceeds $\tilde{C}_l$ near the withdrawal well (for $\tilde{x} > \sim 0.3$). Notwithstanding $\tilde{C}_l < \tilde{C}_v$, contaminant is still transferred from liquid phase to vapor phase as $\tilde{H} = 40$ and hence $\tilde{H}\tilde{C}_l > \tilde{C}_v$ (see equations (41) and (42)). Figure 8 shows that practically all contaminant is removed for most of the region near the entrance. This contaminant is deposited and found near the withdrawal well, where $\tilde{C}_l$ amounts to 2.6. A value of $\tilde{C}_l$ larger than unity implies that C_l exceeds the solubility limit, as seen by (39). This phenomenon will take place if the initial contaminant concentration is high (approximates solubility limit) and/or $\tilde{H}$ is large (more volatile contaminant) and/or Me is large (larger mass transfer rate).

From Figure 8 it can be concluded that for $\tilde{x}$ greater than about 0.95, $\tilde{C}_l$ is larger than unity. This phenomenon is typical of the start-up phase where contaminant is transported in the soil but not removed (in steady state situations, contaminant is removed in the entire region between entrance and withdrawal well). The exceeding of the solubility limit has taken place, first at the steam front as here $\tilde{C}_v$ and $\tilde{C}_l$ are highest, before this front attains the withdrawal well. The present model, however, starts from liquid contaminant concentrations which are below the solubility limit. As soon as the solubility limit is attained in the liquid phase (i.e., $\tilde{C}_l = 1$), the present model loses its validity.

If more contaminant is present than maximum soluble, a free liquid contaminant phase will precipitate. At the liquid side then two phases are present, namely, water saturated with dissolved contaminant and free contaminant. The free contaminant will then first be removed by the steam, the liquid water remaining saturated with contaminant. This distillation of free contaminant has been studied theoretically and experimentally by *Yuan and Udell* [1993]. Under these circumstances the contaminant concentration at the liquid-vapor interface is governed by the pure vapor pressure of the contaminant. In contrast to the present model, where the contaminant concentration at the liquid-vapor interface is related to the

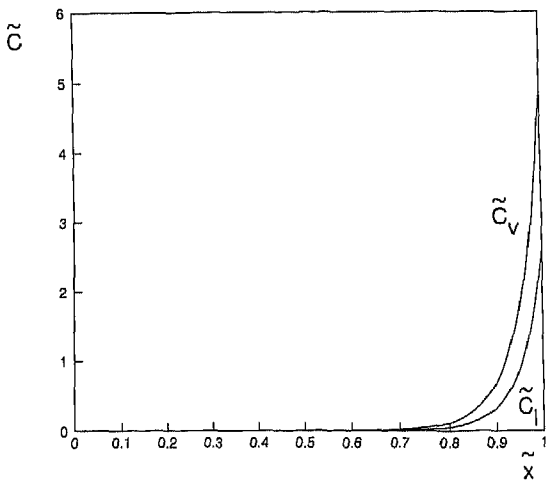

Figure 8. Dimensionless liquid contamination $\tilde{C}_l$ and vapor contamination $\tilde{C}_v$ at the end of the process, $\tilde{C}_{l0} = 0.25$, $\tilde{H} = 400$, $\beta = 0.5$, and $Me = 10^{-1}$.

present liquid contaminant (by Henry's law), the concentration during distillation is constant. As soon as all free contaminant is removed, contaminant will be removed from the liquid water, and hence the present model regains its validity.

It must be stressed that the imposed initial contaminant level, $\bar{C}_{l0} = 0.25$, is rather high. In practice, the dissolved contaminant concentration usually ranges between 0.001 and 0.01 of the solubility limit. Consequently, $\bar{C}_{l0}$ mostly ranges from 0.001 to 0.01. In the case of these much smaller $\bar{C}_{l0}$, the solubility limit will hardly be exceeded, and the present model retains its validity in the entire start-up phase. Table 1 reveals that for $\bar{C}_{l0}$ ranging from 0.001 to 0.01, the drinking water standards are still substantially exceeded. So, for describing the removal of NAPLs to drinking water standards, a model solely based on distillation is not adequate and a model such as presented here should be applied.

Conclusions

The present paper addresses an analysis of steam stripping of the unsaturated zone of subsoils which are contaminated with volatile NAPLs. Particularly, the attention has been focused on the start-up phase. During this phase, steam enters the porous medium and condenses at the steam front, and air initially present in the porous medium is driven out. The contaminant is evaporated and transported behind the front to this front.

First, the propagation of this steam front has been analyzed in some detail. To determine the position, the vapor flow to the front, using Darcy's law, and an energy balance at the front have been used. It is demonstrated that the steam-front position follows $\lambda(a_2 t)^{1/2}$, where λ follows from an implicit algebraic equation. For negligible axial heat loss ahead of the front, λ tends to its maximum value of unity.

Subsequently, the transport of contaminant behind the front is considered. A nonequilibrium model is put forward which involves the transport of the contaminant, which is dissolved in the liquid water phase, to the steam phase. At this front both the contaminant and the steam condense. The governing partial differential equations of the moving boundary problem are transformed and made dimensionless. The resulting system contains three dimensionless numbers, Me, β, and $\tilde{H}$. Me represents the dimensionless mass transfer coefficient, β represents the amount of condensed steam in relation to the total amount of water, and $\tilde{H}$ represents the modified Henry's law coefficient (Henry's law coefficient times the density of liquid water, divided by the density of steam). On the basis of the characteristics of the system, a numerical solution procedure for the transport equations is presented.

For a number of β, $\tilde{H}$, and Me, solutions of the system are computed. During the start-up phase the transport of contaminant from one part of the soil to another is enhanced for larger $\tilde{H}$ and Me. Furthermore, it is seen that under certain circumstances, particularly if the initial contaminant concentration in the liquid phase approximates the solubility limit and/or $\tilde{H}$ and Me are large, the transport and condensation of contaminant are such that the solubility limit can be exceeded. This implies the precipitation of a free contaminant phase and requires an alternative description of the mass transfer, which is then based on distillation. For stripping problems, where the contaminant concentration is low but drinking water standards are exceeded, the present model is adequate.

Notation

a_1 thermal diffusivity [$m^2\ s^{-1}$].
a_2 parameter (equation (24)) [$m^2\ s^{-1}$].
C contaminant concentration [kg m^{-3}].
C_{lm} solubility [kg m^{-3}].
c_p specific heat [J $kg^{-1}\ K^{-1}$].
g_t overall mass transfer coefficient [s^{-1}].
H dimensionless Henry's law coefficient (equation (36)).
$\tilde{H}$ modified dimensionless Henry's law coefficient (equation (45)).
H_{lat} latent heat of condensation [J kg^{-1}].
k thermal conductivity [W $m^{-1}\ K^{-1}$].
L distance between injection and withdrawal wells [m].
M mass of one kilomole of substance [kg].
Me Merkel number (equation (44)).
n number of discretisation points along a coordinate axis.
P pressure [Pa].
R gas constant [J K^{-1} $kmol^{-1}$].
S saturation.
T temperature [K].
t time [s].
u superficial velocity in the direction of x [m s^{-1}].
X_0 position of front between displacing and replaced fluids [m].
x coordinate [m].
y dimensionless group (equation (27)).

Greek symbols

β dimensionless group, (equation (43)).
γ_1, γ_2 parameters [K].
δ distance between discretisation points.
η dynamic viscosity [Pa s].
κ absolute permeability [m^2].
κ_r relative permeability.
λ dimensionless parameter.
ν kinematic viscosity [$m^2\ s^{-1}$].
ρ density [kg m^{-3}].
ϕ porosity.

Subscripts

air pertaining to displaced fluid.
c condensate.
in injection.
ir irreducible.
l liquid.
p contaminant.
s pertaining to solid.
sat saturation.
v pertaining to injected fluid.
0 pertaining to initial condition.

Overbar indicates mean, and tilde indicates transformed.

Acknowledgments. The authors wish to acknowledge the useful discussions with B. H. Gilding of the Faculty of Applied Mathematics. Furthermore, the first author wishes to express his gratitude to H. van Tongeren for his support of this research and to the Cornelis Lely Foundation for its financial support.

References

Bird, R. B., W. E. Stewart, and E. N. Lightfoot, *Transport Phenomena*, John Wiley, New York, 1960.

Buchlin, J. M., and A. Stubos, Phase change phenomena at liquid saturated self heated particulate beds, in *Modelling and Applications of Transport Phenomena in Porous Media*, edited by Jacob Bear and J. M. Buchlin, chap. 3, pp. 221–276, Kluwer Acad., Norwell, Mass., 1991.

Burden, R. L., J. D. Faires, and A. C. Reynolds, *Numerical Analysis*, Prindle, Weber, and Schmidt, Boston, Mass., 1978.

Carslaw, H. S., and J. C. Jaeger, *Conduction of Heat in Solids*, 2nd ed., Clarendon, Oxford, 1959.

Courant, R., and D. Hilbert, *Methods of Mathematical Physics*, vol. I, Wiley-Interscience, New York, 1953.

Falta, R. W., K. Pruess, I. Javandel, and P. A. Witherspoon, Numerical modeling of steam injection for the removal of nonaqueous phase liquids from the subsurface, 1, Numerical formulation, *Water Resour. Res.*, *28*, 443–449, 1992a.

Falta, R. W., K. Pruess, I. Javandel, and P. A. Witherspoon, Numerical modeling of steam injection for the removal of nonaqueous phase liquids from the subsurface, 2, Code validation and application, *Water Resour. Res.*, *28*, 451–465, 1992b.

Gilding, B. H., and S. Li, The parameter dependence of the coefficient in a model for constant-pressure steam injection in soil, *J. Eng. Math.*, in press, 1995.

Hilberts, B., In-situ steamstripping, in *Proceedings of the First International TNO Conference on Contaminated Soil*, edited by J. W. Assink and W. J. van den Brink, pp. 680–686, Morting Nÿhoff, Dordrecht, Netherlands, 1986.

Hunt, J. R., N. Sitar, and K. S. Udell, Nonaqueous phase liquid transport and cleanup, 1, Analysis of mechanisms, *Water Resour. Res.*, *24*, 1247–1258, 1988a.

Hunt, J. R., N. Sitar, and K. S. Udell, Nonaqueous phase liquid transport and cleanup, 2, Experimental studies, *Water Resour. Res.*, *24*, 1259–1269, 1988b.

Maas, J. G., Method of cleaning polluted subsoil and apparatus for carrying out the method, U. K. Patent GB 2098644A, Patent Office, London, 1982.

Miller, C. T., M. M. Poirier-McNeill, and A. S. Mayer, Dissolution of trapped nonaqueous phase liquids: Mass transfer characteristics, *Water Resour. Res.*, *26*, 2783–2796, 1990.

Udell, K. S., and L. D. Stewart, Combined steam injection and vacuum extraction for aquifer cleanup, in *Subsurface Contamination by Immiscible Fluids*, edited by U. Weyer, pp. 327–335, A. A. Balkema, Brookfield, Vt., 1990.

Vreeken, C., and H. T. Sman, Physical techniques for the in situ cleaning of contaminated soil, in *Contaminated Soil '88*, edited by K. Wolf, W. J. van den Brink, and F. J. Colon, pp. 891–900, Kluwer Acad., Norwell, Mass., 1988.

Yuan, Z. G., and K. S. Udell, Steam distillation of a single component hydrocarbon liquid in porous media, *Int. J. Heat Mass Transfer*, *38*, 1965–1976, 1993.

Zauderer, E., *Partial Differential Equations of Applied Mathematics*, 2nd ed., John Wiley, New York, 1989.

H. J. H. Brouwers and S. Li, Department of Civil Engineering and Management, University of Twente, P. O. Box 217, 7500 AE Enschede, Netherlands.

(Received February 6, 1995; accepted April 18, 1995.)